Environmental Science Processes & Impacts

PAPER

View Article Online
View Journal | View Issue

Cite this: *Environ. Sci.: Processes Impacts*, 2022, **24**, 1782

Heteroaggregation of PS microplastic with ferrihydrite leads to rapid removal of microplastic particles from the water column†

Johanna Schmidtmann, *[a] Hassan Elagami,[ab] Bejamin S. Gilfedder,[ab] Jan H. Fleckenstein,[cd] Georg Papastavrou,[e] Ulrich Mansfeld[f] and Stefan Peiffer[a]

Microplastic (MP) particles are ubiquitous in aquatic environments. Therefore, understanding the processes that affect their removal from the water column, such as sedimentation, is critical for evaluating the risk they pose to aquatic ecosystems. We performed sedimentation experiments in which polystyrene (PS) and PS + ferrihydrite, a short-range ordered ferric (oxy)hydroxide, were analyzed in settling columns after 1 day and 1 week of settling time. The presence of ferrihydrite increased sedimentation rates of PS at all pH values studied (pH 3–11). At pH 6 we found that almost all PS particles were removed from the water column after only one day of exposure time. SEM/EDS imaging confirmed heteroaggregation between the PS particles and ferrihydrite. Zeta potential measurements indicated that at acidic pH values the negatively charged PS surface was coated with positively charged ferrihydrite particles leading to charge reversal. Our results demonstrate for the first time that ferric (oxy)hydroxides drive heteroaggregation and subsequent removal of MP from the water column, especially at typical pH values found in natural lake environments. Given their abundance in aquatic systems ferric (oxy)hydroxides need to be regarded as key scavengers of MP.

Received 10th May 2022
Accepted 11th July 2022

DOI: 10.1039/d2em00207h

rsc.li/espi

Environmental significance

The transport and fate of microplastic (MP) particles in the aquatic environment is impacted by interactions of MP with natural particles and colloids. Processes like aggregation or adsorption affect the surface properties of MP particles and their environmental fate and mobility. Here we study the effect of heteroaggregation between MP and ferric(oxy)hydroxide on the sedimentation of MP. Such interactions will be of particular relevance in environmental settings where ferric (oxy)hydroxide particles are abundant, *e.g.* at redox interfaces of aqueous surface and subsurface systems following reoxidation of Fe(II). Such interfaces can arise in groundwater, sediments, wetlands, stratified lakes, and marine environments.

Introduction

Pollution with plastic materials has emerged as one of the most relevant current and future environmental problems.[1–3] Micro- and nanosized particles are of particular concern since they can be taken up by organisms and cells[2,4–6] and may accumulate in the food chain.[7] In the last few years, research focused predominantly on the occurrence and distribution of microplastics (MP) in the environment. Only recently, a more fundamental understanding of microplastic particle behavior in the environment has started to attract attention. Processes like particle aggregation are well known to substantially affect the fate and mobility of particles in the aquatic environment and must therefore be included in modeling transport processes.[1] Heteroaggregation (the aggregation of two or more different colloidal particles) of engineered nanoparticles (ENPs) with natural colloids and suspended solids was shown to strongly affect the aquatic transport and sedimentation of ENPs.[8,9] By contrast, most studies focused on the homoaggregation of MP particles and the influence of pH, electrolytes and natural organic matter (NOM) on this process.[10–18] In the aquatic environment, however, processes triggering heteroaggregation play a much larger role due to the abundance of natural particles and colloids compared to MP particles.[1] Dissolved organic matter has been found to stabilize MP particles

[a]*Department of Hydrology, University of Bayreuth, Germany. E-mail: j.schmidtmann@uni-bayreuth.de*
[b]*Limnological Research Station, University of Bayreuth, Germany*
[c]*Department of Hydrogeology, Helmholtz-Centre for Environmental Research – UFZ, Germany*
[d]*Hydrologic Modelling Unit, University of Bayreuth, Bayreuth, Germany*
[e]*Physical Chemistry II, University of Bayreuth, Germany*
[f]*Bavarian Polymer Institute (BPI), Keylab Electron and Optical Microscopy, University of Bayreuth, Germany*

† Electronic supplementary information (ESI) available. See https://doi.org/10.1039/d2em00207h.

in the aqueous phase by increasing the electrostatic and steric repulsion and to destabilize MP through bridging effects or surface charge reversal.[11,12,14,16,18] Heteroaggregation between MP and biogenic particles was shown to alter the buoyancy of MP and increase its sedimentation rate.[19–22] Despite the abundance and importance of inorganic colloidal material in aquatic systems,[23] studies about the interaction of MP with metal (oxy) hydroxides are scarce. Oriekhova and Stoll (2018) showed that heteroaggregation of polystyrene (PS) at environmental pH is induced by the presence of inorganic colloids (α-Fe_2O_3) and NOM.[24] Furthermore, inorganic coagulants such as polyaluminium chloride (PACl) and aluminium- and iron-based salts have been applied to induce coagulation of MP in aqueous solutions[25] leading to high removal efficiencies of MP particles from the water column.[26,27] In particular, ferric (oxy) hydroxides are abundant in aqueous systems[23,28] and strongly interact with natural organic matter and other water constituents[29–31] to eventually become deposited in sediments and soils.[28,32] Hence, they are a highly relevant aquatic component in respect to heteroaggregation mechanisms in natural aquatic systems. This was also shown by a recent study investigating the aggregation of MP particles with crystalline, poorly crystalline and freshly formed iron oxides.[33] However, to the best of our knowledge no study has been performed on the aggregation and subsequent sedimentation of MP particles with ferric (oxy) hydroxides.

Here, we have studied the aggregation between PS particles and ferrihydrite, a common naturally occurring ferric (oxy) hydroxide.[34] Ferrihydrite has a large surface area (200–300 $m^2\ g^{-1}$)[35] and a pH-dependent surface charge which is usually positively charged in the acidic pH range, negatively charged in the alkaline range and the isoelectric point is typically located at neutral pH.[36] By determining surface properties and aggregate size of PS, ferrihydrite and the formed associates we want to test, if heteroaggregation occurs and how it affects the sedimentation of PS.

Experimental

Selection of polystyrene particles

For the experiments we used spherical PS particles purchased from Microparticles (Berlin, Germany). According to the manufacturer, the particles have a diameter of (1.01 ± 0.03) μm and a density of 1.05 g cm^{-3}. The size and shape of the particles was checked by scanning electron microscopy (*cf.* below). We used a PS concentration of 10 mg L^{-1} (approx. 1.8×10^{10} particles L^{-1}) for the experiments. Comparing the number of particles per volume to plastic concentrations found in the environment, it seems quite high. However, the concentration of plastic particles in the lower micro-meter range (as used in this study) in aquatic environments is not well studied yet.[37] The used concentration is certainly higher than concentration of microplastics found in natural waters, however we had to select a concentration that was sufficiently high enough for the used measurement techniques. Previous studies investigating microplastic interactions and aggregation used concentrations in a similar or often even higher mass per volume ratio (4–160 mg L^{-1}).[11,12,14–16,24,33,38]

Synthesis and characterization of ferrihydrite

The synthesis of ferrihydrite was performed after Cornell and Schwertmann (2003).[23] Two litres of distilled water were preheated to 75 °C to which 20 g unhydrolyzed crystals of $Fe(NO_3)_3 \times 9H_2O$ were added under rapid stirring. The solution was placed for 10 minutes in an oven at 75 °C. The solution was then removed from the oven and rapidly cooled by plunging into iced water. Approximately 30 min later, the solution was transferred to dialysis bags which were placed in distilled water for multiple days. The water was exchanged several times until its conductivity was less than 5 μS cm^{-1}. The reaction product in the dialysis bags was filled into a storage container as soon as the conductivity was <5 μS cm^{-1}[39] and stored at 4 °C.

The synthesis product was analysed for its mineralogy by X-ray powder diffraction (XRD) using a Philips X'Pert Pro diffractometer. The diffractometer was running in reflection mode with monochromated Co$K\alpha_1$ radiation operated at 40 kV and 40 mA in the 2θ range 15°–90° with a step size of 0.02° and scan speed of 0.66° min^{-1}.

For the experiments we used a ferrihydrite concentration of 10 mg L^{-1} which is in the range of iron concentrations in the environment.[40]

Determination of zeta potential and z-averaged hydrodynamic diameter

The zeta potential and the z-averaged hydrodynamic diameter of the PS particles, the ferrihydrite particles as well as the formed heteroaggregates after a reaction time of 1 week were derived from measurements using ZetaSizer Nano ZS (Malvern Panalytical, Germany) by Laser Doppler Electrophoresis or Dynamic Light Scattering (DLS), respectively. A subsample of approx. 1 mL was analyzed at 25 °C using a folded capillary zeta cell (DTS1070, Malvern Panalytical, Germany). Each sample was measured three times. Results are given as average of the individual measurements with standard deviations. All measurements were performed at a concentration of 10 mg L^{-1} PS and 10 mg L^{-1} ferrihydrite, the pH was adjusted to values between 3 and 11 and ionic strength was set to 10 mM by addition of NaCl. Immediately before the ZetaSizer analysis, the samples were briefly shaken to re-suspend any sedimented aggregates.

Sedimentation experiments

To determine the sedimentation rate of PS in the presence of ferrihydrite, we prepared samples with PS (10 mg L^{-1}) and ferrihydrite (10 mg L^{-1}) under standard conditions. The samples with a total volume of 10 mL were prepared in narrow glass vessels (inner diameter ~16 mm). The pH was adjusted to values between 3 and 11 by adding HCl or NaOH. In each vessel, a constant ionic strength of 10 mM was established by addition of adequate amounts of NaCl. After the addition of all reactants, the samples were shaken and allowed to react, one set for 1 day and a second set for 1 week. After 1 day or 1 week the upper 8 mL

of the samples were transferred to a second sample vial without disturbing any settled particles in the lower 2 mL of the sample using a pipette. In the following, we will refer to the lower 2 mL of the sample as sediment and to the upper 8 mL of the sample as solution. Both phases were diluted with ultrapure water (18.2 MΩ cm) to a volume of 9 mL for TOC analysis.

In addition, we also analyzed the sedimentation of PS in the absence of ferrihydrite. For this, we prepared reference samples under identical conditions (pH 3–11 and ionic strength of 10 mM) and PS concentration but without ferrihydrite. After 1 day or 1 week, we removed the upper 8 mL of the samples and analyzed the PS concentration in the upper fraction (solution) and lower fraction (sediment) of the samples.

To determine the PS concentration, we analyzed the samples by thermocatalytic oxidation using a TOC device (TOC-L-Analyzer, Shimadzu, Kyoto, Japan). The presence of Fe species significantly improved the recovery of the PS particles so that 10 mg L^{-1} ferrihydrite was added to all samples before measurement (ESI Fig. S1†). Approx. 10 minutes before the measurement, the samples were acidified with 2 M HCl to dissolve all larger ferrihydrite-aggregates and pre-treated in an ultrasonic bath for 5 minutes. Instead of using the auto sampler of the instruments, the samples were placed on a magnetic stirrer during analysis to prevent sedimentation of the particles.

The PS concentration in sediment and solution was calculated from the measured non-purgeable organic carbon (NPOC) values against a calibration curve (ESI Fig. S1†). Additionally, the recovery of PS was calculated to verify the quality of the method.

Scanning electron microscopy (SEM) and energy-dispersive X-ray spectroscopy (EDS)

Samples were prepared by (i) dropping 4 μL of solution onto a glow-discharged carbon-supported TEM copper grid (S160 Plano, Germany) and (ii) drying under ambient conditions. The samples were coated with a thin layer of platinum by a Cressington 208 HR sputter coater. SEM images were recorded using secondary electron detectors on a Zeiss ULTRA PLUS (Carl Zeiss Microscopy GmbH, Germany) operating at an acceleration voltage of 2 kV. For EDS mapping, the samples were investigated with a Zeiss LEO 1530 (Carl Zeiss Microscopy GmbH, Germany) operating at 2 kV and equipped with an UltraDry EDS detector using Pathfinder software (Thermo Fisher Scientific, USA). EDS resolution was enhanced by use of a thin layer of carbon as specimen support and a low acceleration voltage.

Furthermore, the samples were analyzed using a light microscope and a high 128 definition digital single lens reflex camera (Zeiss Axioplan microscope and Cannon EOS 5D 129 respectively). The advantage of this method is that the samples do not have to be dried but can be analyzed directly in suspension.

Results and discussion

Colloidal properties of polystyrene particles

SEM images revealed spherical, monodisperse particles with a diameter of 1 μm (ESI Fig. S2†) corresponding to the data provided by the manufacturer. The surface of the PS particles was found to be negatively charged over the entire pH range studied. Zeta potentials varied from (-44.0 ± 0.7) mV at pH 3 to (-82.9 ± 5.6) mV at pH 11 (Fig. 1A). The z-averaged hydrodynamic diameter of the PS particles was (1.70 ± 0.15) μm and did not show a trend or significant variations over the pH range (Fig. 1B). Even though the relatively negative zeta potential indicates a strong electrostatic repulsion some aggregates must have formed during storage. This interpretation is in-line with the presence of a detectable sediment, which we consider in the following as reference value for sedimentation of the bare particles.

Sedimentation analysis of the reference samples shows that the PS concentrations in the sediment were rather constant over the pH range and no trend was observed. Fig. 2 displays the percentage of all PS found in the sediment of a sample after 1 day or 1 week of settling time. After a settling time of 1 day, the mean PS concentration in the sediment (11.27 ± 1.31) mg L^{-1} was slightly higher compared to the solution (8.85 ± 0.56) mg L^{-1}. After 1 week, the concentration in the sediment clearly increased to a mean of (21.20 ± 2.24) mg L^{-1}, whereas the PS concentration in the solution was reduced to (7.17 ± 0.64) mg L^{-1}. In a well-mixed dispersion where no sedimentation would take place, 20% of the total PS in the sample should be found in the sediment (bottom 2 mL). However, after 1 day, between 20.4% and 27.9% of the initially added particles were recovered in the sediment and between 34.4% and 47.8% after 1 week. Hence, although highly negative zeta potentials suggest that the PS particles should be stable in dispersion, the sedimentation study indicates that some PS particles tend to homoaggregate and to sediment under the analyzed conditions (10 mM NaCl). This agrees well with a recent study examining the aggregation of exactly the same 1 μm PS particles using spICP-MS.[41] There it was found that 63% of PS particles did not aggregate, 25% were found in aggregates of two particles and the remaining 12% in aggregates of more than 2 particles. The increase in the fraction of sedimented PS from 1 day to 1 week suggests an unknown kinetic control on the sedimentation process. As no pH dependence for the sedimentation has been observed, we attribute the sedimentation primarily to long-term storage effects.

Colloidal properties of ferrihydrite

The X-ray diffractogram of the synthesized ferric (oxy)hydroxide shows six broadened lines (ESI Fig. S3†) characteristic for 6-line ferrihydrite.[23] The isoelectric point (pH_{IEP}) is located at pH ≈ 8.7 (Fig. 1A) and thus slightly higher than values reported in the literature ($pH_{IEP} \approx 7$).[36,42] At pH values < 6, ferrihydrite particles were in nanometer size range and part of the iron (oxy) hydroxides might even be present as dissolved iron. In these samples, count rates were not sufficient for reliable light scattering measurements. Therefore, the zeta potential and z-averaged hydrodynamic diameter results of ferrihydrite samples at pH < 6 have no quantitative value but provide a reasonable estimate for pH_{IEP}. However, based on previously reported findings, we can safely assume that the zeta potential

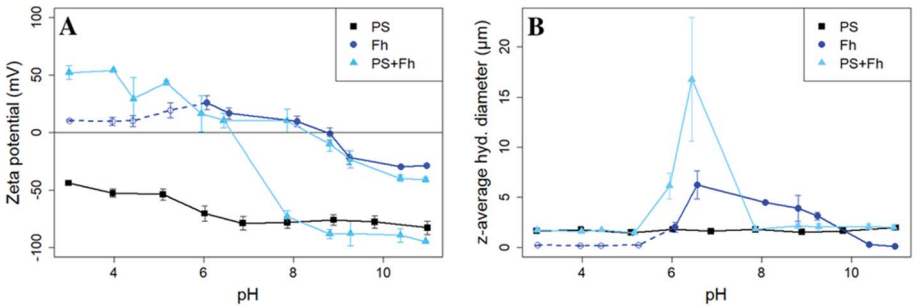

Fig. 1 Zeta potential (A) and z-average hydrodynamic diameter (B) of PS (10 mg L^{-1}, I = 10 mM, black squares), ferrihydrite (Fh, 10 mg L^{-1}, I = 10 mM, darkblue circles), and samples with PS + ferrihydrite (PS + Fh, 10 mg L^{-1} PS, 10 mg L^{-1} Fh, I = 10 mM, lightblue triangles). For ferrihydrite samples with pH < 6, the count rates were not sufficient for reliable light scattering measurements and therefore should be regarded with caution (dashed darkblue line). For samples with PS + ferrihydrite (lightblue) at pH > 7.9 two trajectories of the zeta potential are displayed, because the zeta potential distribution showed not one but two distinct zeta potential peaks (ESI Fig. S4†).

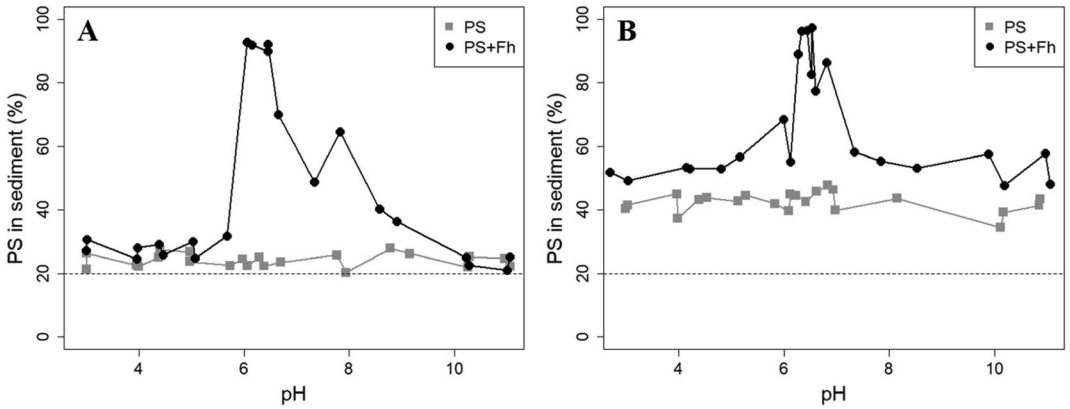

Fig. 2 Percentage of PS found in the sediment of the samples after a settling time of (A) 1 day and (B) 1 week. The grey curve shows the reference samples in which only PS is present, and the black curve shows the samples in which PS and ferrihydrite (PS + Fh) is present. In a well-mixed dispersion where no sedimentation takes place, 20% of the total PS in the sample should be found in the sediment (dashed line).

values of ferrihydrite for pH 3–6 will be positive and increase with decreasing pH.[42]

For pH values between 6 and 9, we notice an increase in the z-averaged hydrodynamic diameter up to a maximum of (6.26 ± 1.42) µm at pH 6.6. The size maximum is not located at the pH_{IEP}. However, the repulsive forces between the particles at the pH of maximum homoaggregation may already be so weak that aggregation takes place. The relatively low zeta potential (Ψ_{zeta} = 16.8 mV) is in line with this interpretation. For samples with a pH > 10, the absolute value of the zeta potential increases again to approx. −30 mV and the z-averaged hydrodynamic diameter is decreasing again to values less than 0.3 µm.

Heteroaggregation and subsequent sedimentation of polystyrene and ferrihydrite

The presence of ferrihydrite leads to substantial increases of the sedimentation rate of PS relative to the rates observed in the reference samples without ferrihydrite, particularly after an exposure time of 1 week (Fig. 2). After 1 day, moderate sedimentation of PS of about 25% of the initially added particles was observed in the acidic (pH < 6) and alkaline range (pH > 9), both in the presence and absence of ferrihydrite. However, at pH values between 6 and 9, the presence of ferrihydrite induced a distinct increase in sedimentation with maximum sedimentation rates between pH 6 and 6.5. In this pH range 90–93% of the PS were found in the sediment after settling. After 1 week, the maximum sedimentation rate (83–97%) of PS particles was found at the same pH range. For all other pH values (pH 3–6 & 7–11), the sedimentation rate of PS in the presence of ferrihydrite increased to 50–60% compared to the sedimentation rate observed after 1 day (with the exception of pH value 7.8). In these pH ranges, sedimentation rates were distinctly higher than those observed in the absence of ferrihydrite. Taken together, these observations point to heteroaggregation between PS particles and ferrihydrite and subsequent sedimentation of these heteroaggregates with a maximum at pH ~6.5.

Interestingly, the characteristic negative surface charge of PS can no longer be identified in the acidic pH range (Fig. 1A). Instead, the zeta potential values are positive with a maximum of (54.1 ± 0.2) mV at pH 4. Therefore, it seems likely that the positively charged ferrihydrite adsorbed to the PS particles which in consequence reversed their negative charge. This is confirmed by EDS mapping of the samples at pH 4 which shows

a surface coating of the PS particles with ferrihydrite (Fig. 3). Similar observations were reported by Li *et al.* (2019) who demonstrated that, depending on the size of the PS particles, iron oxides adsorbed onto the surface of PS or *vice versa*.[43] The smaller sized colloidal objects always adsorbed onto the larger ones. Given the small particle sizes of ferrihydrite colloids observed at acidic pH (Fig. 1B), it therefore seems likely that they adsorbed onto the significantly larger PS particles at these pH conditions. Due to the small size of the ferrihydrite particles compared to the PS, no obvious change in dimensions of the overall particles can be observed (Fig. 2B and 3, ESI Fig. S5A†). The particle size of the heteroaggregates in the acidic pH range is similar to that of the pure PS particles, however with a distinctly different charge. Due to the substantially higher density of ferrihydrite particles (3.9 g cm^{-3})[44] as compared to PS particles (1.05 g cm^{-3}), already very small ferrihydrite particles adsorbed onto the PS surface may lead to the observed increase in sedimentation rate of the PS-ferrihydrite heteroaggregates in the acidic pH range by a factor of 1.3.

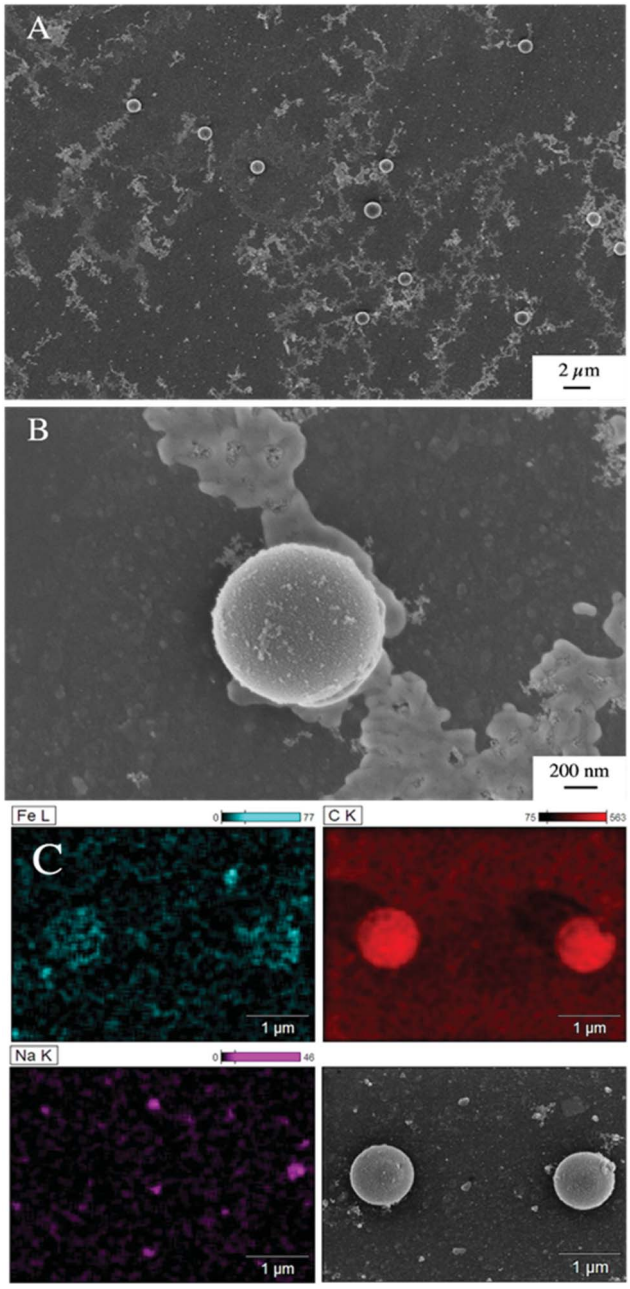

Fig. 3 SEM images of a sample with PS and ferrihydrite at pH 4 showing isolated PS particles and statistically distributed, nano-sized ferrihydrite besides larger agglomerates of dried sodium salt (A). At higher magnification, a coating of the PS particles can be observed (B). EDS analysis indicates a higher iron concentration on the PS particles compared to the carbon background (C).

For samples with pH > 7.9 we identified not one but two distinct peaks in the zeta potential distribution (ESI Fig. S4†). Therefore, two different trajectories of the zeta potential for pH > 7.9 are plotted for the PS-ferrihydrite heteroaggregates (Fig. 1A). One of the trajectories follows the course of the zeta potentials determined for reference PS particles, while the other trajectory matches the zeta potential measurements of unreacted ferrihydrite. We assume that this observation is due to the co-occurrence of PS and ferrihydrite particles that stay separated and that no (major) adsorption and subsequent heteroaggregation takes place in the alkaline range (ESI Fig. S5C†). Since two different types of particles with different sizes are present at this pH range, the results of the z-averaged hydrodynamic diameter are not considered to be very reliable for the alkaline range. Despite their negative charge, sedimentation rates of PS particles in the presence of ferrihydrite are also enhanced at alkaline pH values compared to the sedimentation rates determined in the absence of ferrihydrite. Similar observations were made by Li *et al.* (2019) who were able to demonstrate that the addition of suspended sediment to a suspension of 100 nm PS particles enhances the settling rate of PS at 50 mM NaCl, although both particle types were negatively charged.[38] Aggregation despite apparent electrostatic repulsion has also been described in previous studies and was related to discrete nanoscale surface heterogeneity.[45,46] Therefore, we assume that some particles aggregate despite repulsive forces and therefore cause the amplified sedimentation of PS in presence of ferrihydrite in the alkaline range.

Low, slightly positive zeta potentials (Fig. 1A) were found at circumneutral pH values (between 6 and 8). Such minimum coincides with a very large peak of the z-averaged hydrodynamic diameter of above 15 μm at pH 6.4 (Fig. 1B), which underpins heteroaggregation of several particles. The numerical value of the z-averaged hydrodynamic diameter needs to be regarded as a rough estimate, though. The instrument used here can determine particle diameters only up to a size of 10 μm by DLS. However, SEM and light microscopy show that the aggregate dimensions clearly exceed this limit. Hence, our data indicate that strong heteroaggregation is taking place at pH 6–7 and heteroaggregates with dimensions of more than 10 μm have been formed. Optical microscopy imaging revealed aggregates with sizes ranging from a few micrometers up to 100 μm (ESI Fig. S5B†). Formation of heteroaggregates is further corroborated by SEM images of samples at pH 6.5 (Fig. 4) with EDS analysis clearly showing that ferrihydrite adsorbs on PS particles and connects the PS particles to larger aggregates (Fig. 4C).

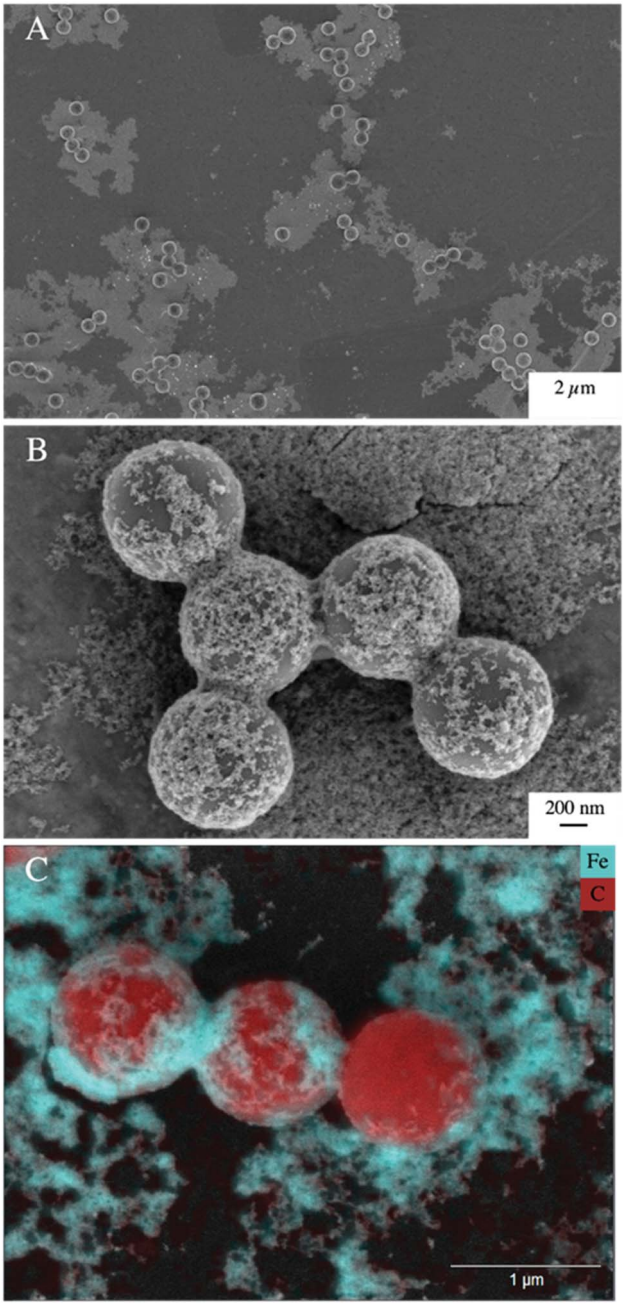

Fig. 4 SEM image of formed heteroaggregates of PS and ferrihydrite at pH 6.5 shows the locally coinciding agglomeration of ferrihydrite and PS particles (A). Higher magnification indicates the ferrihydrite on the surface of and linkages between the PS (B). EDS analysis confirms that the adsorbed/aggregated material on the PS is ferrihydrite (C).

This pH is close to the isoelectric point of ferrihydrite. Similarly, Oriekova and Stoll (2018) observed heteroaggregation of PS nanoplastic with α-Fe_2O_3 particles at pH 8 under varying PS concentrations to occur at PS concentration levels at which the isoelectric point of the mixtures is achieved.[24] Vu *et al.* (2022) observed maximal heteroaggregation of PS and ferrihydrite to occur at pH values at which the surface charge of ferrihydrite is rather low.[33] We therefore propose that the surface charge of MP becomes neutralized upon adsorption of neutral or weakly charged iron colloids leading to an increase of van der Waals attraction forces and subsequent aggregation.[33]

Conclusions

Previous studies have demonstrated heteroaggregation of MP particles and their subsequent removal from the water column with phytoplankton,[20,22] microalgae,[19] suspended sediment[38] or calcite.[47] In this study, we demonstrate for the first time that the presence of ferric iron particles is driving not only heteroaggregation[24,33] but also sedimentation of MP at rates at which almost all PS was found in the sediment already after 1 day of settling. The interactions between PS and ferrihydrite were strongly pH dependent. At acidic pH a coating of the negative PS surface by positively charged ferrihydrite was observed due to strong electrostatic attraction which led to charge reversal. In contrast, no major aggregation took place in the alkaline pH range due to repulsive forces between PS and ferrihydrite. At circumneutral pH, charge neutralization resulted in the formation of large heteroaggregates which subsequently sedimented to the bottom of the sample vial. Irrespective of their idealized shape and their smooth surface, the PS particles analyzed in this study can be regarded as model substances for other MP particles.

Environmental processes, such as UV exposure[48] or the formation of biofilms on the surface will even increase surface reactivity of MP particles[21] so that interactions between ferric (oxy)hydroxides and MP may be even more pronounced. However, removal of MP particles upon interaction with ferric (oxy)hydroxides from the water surface to deeper water compartments at a time scale of days may also reduce the exposure time to UV radiation.

Overall, our research suggests that MP particles will tend to form an environmental corona at their surface consisting of ferric (oxy)hydroxides but also of other constituents[49,50] once entering aqueous systems that affects their environmental behaviour. Removal of MP from the water column following heteroaggregation with ferric (oxy)hydroxides will reduce exposure times of aquatic organisms to MP.[51,52] Inversely it may cause a higher risk for organisms in the benthic zone since lake and river sediments may act as a sink for MP particles.[38,53,54] Moreover, ferric iron induced heteroaggregation of MP particles may be considered an interesting process for MP removal in waste-water treatment systems.

Data availability

The datasets used in this study are published on Zenodo at **https://doi.org/10.5281/zenodo.6855575**.

Conflicts of interest

There are no conflicts to declare.

Acknowledgements

The study was funded by the Deutsche Forschungsgemeinschaft (DFG, German Research Foundation) –

Project Number 391977956 – SFB 1357 Microplastics. The authors would like to thank Martina Heider for taking SEM images at the Bavarian Polymer Institute (BPI), Tiziana Boffa Ballaran for XRD analysis at the Bavarian Research Institute of Experimental Geochemistry and Geophysics (BGI) and Laura Wegner and Jutta Eckert for their help with TOC measurements.

References

1 O. S. Alimi, J. Farner Budarz, L. M. Hernandez and N. Tufenkji, Microplastics and nanoplastics in aquatic environments: aggregation, deposition, and enhanced contaminant transport, *Environ. Sci. Technol.*, 2018, **52**, 1704–1724.

2 K. Duis and A. Coors, Microplastics in the aquatic and terrestrial environment: sources (with a specific focus on personal care products), fate and effects, *Environ. Sci. Eur.*, 2016, **28**, 2.

3 R. C. Thompson, Y. Olsen, R. P. Mitchell, A. Davis, S. J. Rowland, A. W. John, D. McGonigle and A. E. Russell, Lost at sea: where is all the plastic?, *Science*, 2004, **304**, 838.

4 A. F. R. M. Ramsperger, J. Jasinski, M. Völkl, T. Witzmann, M. Meinhart, V. Jérôme, W. P. Kretschmer, R. Freitag, J. Senker, A. Fery, H. Kress, T. Scheibel and C. Laforsch, Supposedly identical microplastic particles substantially differ in their material properties influencing particle-cell interactions and cellular responses, *J. Hazard. Mater.*, 2022, **425**, 127961.

5 J. Rudolph, M. Völkl, V. Jérôme, T. Scheibel and R. Freitag, Noxic effects of polystyrene microparticles on murine macrophages and epithelial cells, *Sci. Rep.*, 2021, **11**, 15702.

6 S. L. Wright, R. C. Thompson and T. S. Galloway, The physical impacts of microplastics on marine organisms: a review, *Environ. Pollut.*, 2013, **178**, 483–492.

7 K. Cverenkárová, M. Valachovičová, T. Mackuľak, L. Žemlička and L. Bírošová, Microplastics in the Food Chain, *Life*, 2021, **11**, 1349.

8 A. Praetorius, J. Labille, M. Scheringer, A. Thill, K. Hungerbühler and J.-Y. Bottero, Heteroaggregation of Titanium Dioxide Nanoparticles with Model Natural Colloids under Environmentally Relevant Conditions, *Environ. Sci. Technol.*, 2014, **48**, 10690–10698.

9 I. Velzeboer, J. T. K. Quik, D. van de Meent and A. A. Koelmans, Rapid settling of nanoparticles due to heteroaggregation with suspended sediment, *Environ. Toxicol. Chem.*, 2014, **33**, 1766–1773.

10 A. Abdurahman, K. Cui, J. Wu, S. Li, R. Gao, J. Dai, W. Liang and F. Zeng, Adsorption of dissolved organic matter (DOM) on polystyrene microplastics in aquatic environments: Kinetic, isotherm and site energy distribution analysis, *Ecotoxicol. Environ. Saf.*, 2020, **198**, 110658.

11 L. Cai, L. Hu, H. Shi, J. Ye, Y. Zhang and H. Kim, Effects of inorganic ions and natural organic matter on the aggregation of nanoplastics, *Chemosphere*, 2018, **197**, 142–151.

12 S. Li, H. Liu, R. Gao, A. Abdurahman, J. Dai and F. Zeng, Aggregation kinetics of microplastics in aquatic environment: Complex roles of electrolytes, pH, and natural organic matter, *Environ. Pollut.*, 2018, **237**, 126–132.

13 T. Oncsik, G. Trefalt, Z. Csendes, I. Szilagyi and M. Borkovec, Aggregation of Negatively Charged Colloidal Particles in the Presence of Multivalent Cations, *Langmuir*, 2014, **30**, 733–741.

14 A. Pradel, S. Ferreres, C. Veclin, H. El Hadri, M. Gautier, B. Grassl and J. Gigault, Stabilization of Fragmental Polystyrene Nanoplastic by Natural Organic Matter: Insight into Mechanisms, *ACS EST Water*, 2021, **1**, 1198–1208.

15 N. Singh, E. Tiwari, N. Khandelwal and G. K. Darbha, Understanding the stability of nanoplastics in aqueous environments: effect of ionic strength, temperature, dissolved organic matter, clay, and heavy metals, *Environ. Sci.: Nano*, 2019, **6**, 2968–2976.

16 J. Wang, X. Zhao, A. Wu, Z. Tang, L. Niu, F. Wu, F. Wang, T. Zhao and Z. Fu, Aggregation and stability of sulfate-modified polystyrene nanoplastics in synthetic and natural waters, *Environ. Pollut.*, 2020, 114240.

17 J. Wu, R. Jiang, W. Lin and G. Ouyang, Effect of salinity and humic acid on the aggregation and toxicity of polystyrene nanoplastics with different functional groups and charges, *Environ. Pollut.*, 2019, **245**, 836–843.

18 S. Yu, M. Shen, S. Li, Y. Fu, D. Zhang, H. Liu and J. Liu, Aggregation kinetics of different surface-modified polystyrene nanoparticles in monovalent and divalent electrolytes, *Environ. Pollut.*, 2019, **255**, 113302.

19 F. Lagarde, O. Olivier, M. Zanella, P. Daniel, S. Hiard and A. Caruso, Microplastic interactions with freshwater microalgae: Hetero-aggregation and changes in plastic density appear strongly dependent on polymer type, *Environ. Pollut.*, 2016, **215**, 331–339.

20 M. Long, B. Moriceau, M. Gallinari, C. Lambert, A. Huvet, J. Raffray and P. Soudant, Interactions between microplastics and phytoplankton aggregates: Impact on their respective fates, *Mar. Chem.*, 2015, **175**, 39–46.

21 J. Michels, A. Stippkugel, M. Lenz, K. Wirtz and A. Engel, Rapid aggregation of biofilm-covered microplastics with marine biogenic particles, *Proc. R. Soc. B*, 2018, **285**, 20181203.

22 P. Möhlenkamp, A. Purser and L. Thomsen, Plastic microbeads from cosmetic products: an experimental study of their hydrodynamic behaviour, vertical transport and resuspension in phytoplankton and sediment aggregates, *Elem. Sci. Anth.*, 2018, **6**, DOI: **10.1525/elementa.317**.

23 R. M. Cornell and U. Schwertmann, *The Iron Oxides: Structure, Properties, Reactions, Occurrences and Uses*, John Wiley & Sons, 2003.

24 O. Oriekhova and S. Stoll, Heteroaggregation of nanoplastic particles in the presence of inorganic colloids and natural organic matter, *Environ. Sci.: Nano*, 2018, **5**, 792–799.

25 W. He, Z. Xie, W. Lu, M. Huang and J. Ma, Comparative analysis on floc growth behaviors during ballasted flocculation by using aluminum sulphate (AS) and polyaluminum chloride (PACl) as coagulants, *Sep. Purif. Technol.*, 2019, **213**, 176–185.

26 Y. Gong, Y. Bai, D. Zhao and Q. Wang, Aggregation of carboxyl-modified polystyrene nanoplastics in water with aluminum chloride: Structural characterization and theoretical calculation, *Water Res.*, 2022, **208**, 117884.
27 G. Zhou, Q. Wang, J. Li, Q. Li, H. Xu, Q. Ye, Y. Wang, S. Shu and J. Zhang, Removal of polystyrene and polyethylene microplastics using PAC and FeCl3 coagulation: Performance and mechanism, *Sci. Total Environ.*, 2020, 141837.
28 B. Lo and T. D. Waite, Structure of Hydrous Ferric Oxide Aggregates, *J. Colloid Interface Sci.*, 2000, **222**, 83–89.
29 H. J. Curtinrich, S. D. Sebestyen, N. A. Griffiths and S. J. Hall, Warming Stimulates Iron-Mediated Carbon and Nutrient Cycling in Mineral-Poor Peatlands, *Ecosystems*, 2022, **25**, 44–60.
30 K. G. J. J. Nierop, B. Jansen and J. M. Verstraten, Dissolved organic matter, aluminium and iron interactions: precipitation induced by metal/carbon ratio, pH and competition, *Sci. Total Environ.*, 2002, **300**, 201–211.
31 S. Peiffer, K. Walton-Day and D. L. Macalady, The Interaction of Natural Organic Matter with Iron in a Wetland (Tennessee Park, Colorado) Receiving Acid Mine Drainage, *Aquat. Geochem.*, 1999, **5**, 207–223.
32 K. Lalonde, A. Mucci, A. Ouellet and Y. Gélinas, Preservation of organic matter in sediments promoted by iron, *Nature*, 2012, **483**, 198–200.
33 T. T. T. Vu, P. H. Nguyen, T. V. Pham, P. Q. Do, T. T. Dao, A. D. Nguyen, L. Nguyen-Thanh, V. M. Dinh and M. N. Nguyen, Comparative effects of crystalline, poorly crystalline and freshly formed iron oxides on the colloidal properties of polystyrene microplastics, *Environ. Pollut.*, 2022, **306**, 119474.
34 E. Jansen, A. Kyek, W. Schäfer and U. Schwertmann, The structure of six-line ferrihydrite, *Appl. Phys. A*, 2002, **74**, 1004–1006.
35 U. Schwertmann and R. M. Cornell, *Iron Oxides in the Laboratory: Preparation and Characterization*, John Wiley & Sons Ltd, Weinheim, 2008.
36 M. Kosmulski, Isoelectric points and points of zero charge of metal (hydr)oxides: 50years after Parks' review, *Adv. Colloid Interface Sci.*, 2016, **238**, 1–61.
37 J. L. Conkle, C. D. Báez Del Valle and J. W. Turner, Are We Underestimating Microplastic Contamination in Aquatic Environments?, *Environ. Manage.*, 2018, **61**, 1–8.
38 Y. Li, X. Wang, W. Fu, X. Xia, C. Liu, J. Min, W. Zhang and J. C. Crittenden, Interactions between nano/micro plastics and suspended sediment in water: Implications on aggregation and settling, *Water Res.*, 2019, **161**, 486–495.
39 L. Gentile, T. Wang, A. Tunlid, U. Olsson and P. Persson, Ferrihydrite Nanoparticle Aggregation Induced by Dissolved Organic Matter, *J. Phys. Chem. A*, 2018, **122**, 7730–7738.
40 A. Kappler, C. Bryce, M. Mansor, U. Lueder, J. M. Byrne and E. D. Swanner, An evolving view on biogeochemical cycling of iron, *Nat. Rev. Microbiol.*, 2021, **19**, 360–374.
41 M. Mansor, S. Drabesch, T. Bayer, A. Van Le, A. Chauhan, J. Schmidtmann, S. Peiffer and A. Kappler, Application of Single-Particle ICP-MS to Determine the Mass Distribution and Number Concentrations of Environmental Nanoparticles and Colloids, *Environ. Sci. Technol. Lett.*, 2021, **8**, 589–595.
42 J. Liu, S. M. Louie, C. Pham, C. Dai, D. Liang and Y. Hu, Aggregation of ferrihydrite nanoparticles: Effects of pH, electrolytes,and organics, *Environ. Res.*, 2019, **172**, 552–560.
43 M. Li, L. He, M. Zhang, X. Liu, M. Tong and H. Kim, Cotransport and Deposition of Iron Oxides with Different-Sized Plastic Particles in Saturated Quartz Sand, *Environ. Sci. Technol.*, 2019, **53**, 3547–3557.
44 T. Hiemstra and W. H. Van Riemsdijk, A surface structural model for ferrihydrite I: Sites related to primary charge, molar mass, and mass density, *Geochim. Cosmochim. Acta*, 2009, **73**, 4423–4436.
45 A. Al Harraq and B. Bharti, Microplastics through the Lens of Colloid Science, *ACS Environ. Au*, 2021, **2**, 3–10, DOI: **10.1021/acsenvironau.1c00016**.
46 I. L. Molnar, W. P. Johnson, J. I. Gerhard, C. S. Willson and D. M. O'Carroll, Predicting colloid transport through saturated porous media: A critical review, *Water Resour. Res.*, 2015, **51**, 6804–6845.
47 R. Leiser, R. Jongsma, I. Bakenhus, R. Möckel, B. Philipp, T. R. Neu and K. Wendt-Potthoff, Interaction of cyanobacteria with calcium facilitates the sedimentation of microplastics in a eutrophic reservoir, *Water Res.*, 2021, **189**, 116582.
48 N. Meides, T. Menzel, B. Poetzschner, M. G. J. Löder, U. Mansfeld, P. Strohriegl, V. Altstaedt and J. Senker, Reconstructing the Environmental Degradation of Polystyrene by Accelerated Weathering, *Environ. Sci. Technol.*, 2021, **55**, 7930–7938.
49 T. S. Galloway, M. Cole and C. Lewis, Interactions of microplastic debris throughout the marine ecosystem, *Nat. Ecol. Evol.*, 2017, **1**, 116.
50 A. F. R. M. Ramsperger, V. K. B. Narayana, W. Gross, J. Mohanraj, M. Thelakkat, A. Greiner, H. Schmalz, H. Kress and C. Laforsch, Environmental exposure enhances the internalization of microplastic particles into cells, *Sci. Adv.*, 2020, **6**, eabd1211.
51 S. Franzellitti, L. Canesi, M. Auguste, R. H. G. R. Wathsala and E. Fabbri, Microplastic exposure and effects in aquatic organisms: A physiological perspective, *Environ. Toxicol. Pharmacol.*, 2019, **68**, 37–51.
52 H. Elagami, P. Ahmadi, J. H. Fleckenstein, S. Frei, M. Obst, S. Agarwal and B. S. Gilfedder, Measurement of microplastic settling velocities and implications for residence times in thermally stratified lakes, *Limnol. Oceanogr.*, 2022, **67**, 934–945.
53 P. Näkki, O. Setälä and M. Lehtiniemi, Seafloor sediments as microplastic sinks in the northern Baltic Sea – Negligible upward transport of buried microplastics by bioturbation, *Environ. Pollut.*, 2019, **249**, 74–81.
54 S. Zhao, J. E. Ward, M. Danley and T. J. Mincer, Field-Based Evidence for Microplastic in Marine Aggregates and Mussels: Implications for Trophic Transfer, *Environ. Sci. Technol.*, 2018, **52**, 11038–11048.